

Training effect in specular spin valves

J. Ventura,^{*} J. P. Araujo, and J. B. Sousa[†]

IN, IFIMUP unit and Faculty of Sciences, Universidade do Porto, Rua do Campo Alegre, 678, 4169-007 Porto, Portugal

A. Veloso and P. P. Freitas[‡]

IN, INESC-MN unit and IST, Rua Alves Redol, 9-1, 1000-029 Lisbon, Portugal

(Received 28 July 2007; revised manuscript received 2 April 2008; published 5 May 2008)

Specular spin valves show an enhanced giant magnetoresistive (GMR) ratio due to specular reflection in nano-oxide layers (NOLs) formed by the partial oxidation of CoFe pinned and free layers. The oxides that form the (pinned layer) NOL were recently shown to antiferromagnetically order at $T \sim 175$ K. Here, we study the training effect (TE) in MnIr/CoFe/NOL/CoFe/Cu/CoFe/NOL/Ta specular spin valves in the 300–15 K temperature range. The exchange bias direction between the MnIr and CoFe layers impressed during annealing is taken as the positive direction. The training effect is observed in antiferromagnetic (AFM)/ferromagnetic (FM) exchange systems and related to the rearrangement of interfacial AFM spin structure with the number of hysteretic cycles performed (n), resulting in the decrease of the exchange field (H_{exch}). Here, in the studied specular spin valve, TE was only observed for $T < 175$ K and is thus related to the pinned layer NOL-AFM ordering and to the evolution of the corresponding spin structure with n . We show that FM spins that are strongly coupled to AFM domains do not align with the applied positive magnetic field (H), giving rise to a residual MR at $H \gg 0$. Such nonsaturating MR will be related with a spin-glass-like behavior of the interfacial magnetism induced by the nano-oxide layer. The observed dependence of the training effect on the field cooling procedure is also likely associated with the existence of different spin configurations available in the magnetically disordered oxide. Furthermore, anomalous magnetoresistance cycles measured after cooling runs under -500 Oe are here related to induced NOL exchange bias/applied magnetic field misalignment. The temperature dependence of the training effect was obtained and fitted by using a recent theoretical model.

DOI: [10.1103/PhysRevB.77.184404](https://doi.org/10.1103/PhysRevB.77.184404)

PACS number(s): 75.70.Cn, 75.70.Kw, 73.43.Qt, 75.47.De

I. INTRODUCTION

When a ferromagnetic (FM) layer is just adjacent to an antiferromagnet, the hysteresis loop of the ferromagnet is shifted from zero magnetic field^{1,2} by an amount known as the exchange field (H_{exch}). Furthermore, an enhanced ferromagnet coercivity is always observed in such antiferromagnetic (AFM)/FM systems. The exchange bias effect occurs after field cooling below the Néel temperature (T_N) of the antiferromagnet. Although known for several decades, the microscopic origin of the exchange bias effect is still controversial. The original model of Meiklejohn and Bean¹ assumed a perfect uncompensated AFM surface. This model, however, predicts H_{exch} values that are orders of magnitude larger than those experimentally observed. Other models^{3–5} suggest that a domain wall parallel to the interface is formed in the AFM layer during the FM magnetization reversal. Therefore, a minimum antiferromagnet thickness (ranging from 25 to 100 Å) for the occurrence of exchange bias is necessary. Although they give correct H_{exch} values, these models predict zero exchange bias if the motion of the AFM spins is not restricted to a plane parallel to the film and exchange bias occurs only if uncompensated AFM spins are assumed at the interface.⁶

Another theoretical approach takes into account the roughness at the AFM/FM interface and the presence of random-exchange interactions between the FM and AFM spins. This gives rise to the formation of domains in the antiferromagnet perpendicular to the interface and also to correct exchange field values and enhanced coercivity.^{7,8} The domain state model^{9–11} considers that the magnetization of

the AFM layer is divided into multidomains, not only at the interface, but through the bulk of the AFM layer, giving rise to a net surface magnetization at the AFM/FM interface that controls the exchange bias. In fact, when cooling below T_N in the presence of an applied magnetic field H , the magnetization of the FM layer (aligned with H) will induce, through an exchange interaction, a net surface AFM spin structure in such favored direction. The exchange field and the enhanced coercivity are then attributed to AFM domains that, due to a high local AFM anisotropy, do not flip and to those that (having weaker local anisotropy) reverse with the switching of the FM magnetization. A more recent model¹² suggests that interface disorder, which arises from roughness, deviations from stoichiometry, defects, or low spin coordination at surface sites, leads to domains and domain walls at the AFM/FM interface,¹³ with spin-glass-like characteristics. Upon cooling, it is argued that uncompensated spins with large AFM anisotropy become frozen and give rise to an exchange bias, while the coercivity enhancement arises from interfacial spins with reduced AFM anisotropy.

Many exchange bias theories then rely on the existence of uncompensated spins at the AFM interface as the origin of the coupling mechanism. Recent results indeed suggest that a small number of uncompensated AFM spins at the interface might be the origin of the loop shift^{14–17} and a linear relation between the amount of net frozen spins and the exchange bias field was observed.¹⁸

Another effect that sometimes arises in AFM/FM exchange systems is the so-called training effect (TE). This consists of the change in both the descending and the ascending switching fields of the hysteresis loops with the number

of cycles performed (n), resulting in the decrease in the exchange and coercive fields. The hysteresis loop shape is also altered due to a change in the reversal mechanism with n .^{19–21} This effect is explained as the rearrangement of the (metastable) spin structure of the AFM layer with each reversal of the magnetization of the FM layer. This leads to a partial loss of its (AFM layer) net magnetization (M) and, thus, in a reduction of the exchange bias. Such M loss with cycling was recently shown to occur in exchange biased NiO/Fe bilayers.²² Thus, the TE reflects the nonequilibrium AFM configuration of the field cooled state.

The dependence of the exchange field with the number of cycles performed (for $n > 1$) usually follows the empirical relation^{22,23}

$$H_{\text{exch}}^n - H_{\text{exch}}^\infty = \frac{\kappa}{\sqrt{n}}, \quad (1)$$

where H_{exch}^n (H_{exch}^∞) is the exchange field at the n th cycle (in the limit of an infinite number of cycles) and κ is a system dependent constant. The power law behavior of Eq. (1) does not hold for $n=1$, a fact that is usually attributed to the difference between the dominant FM layer reversal mechanisms for $n=1$ and $n \geq 2$: domain wall movement and coherent magnetization rotation, respectively. A more elaborated and solid theoretical basis for Eq. (1) was given by Binek,²³ who, based on free energy considerations, arrived at the recursive equation

$$H_{\text{exch}}^{n+1} - H_{\text{exch}}^n = -\gamma(H_{\text{exch}}^n - H_{\text{exch}}^\infty)^3. \quad (2)$$

This relation is valid for $n \geq 1$ and goes into Eq. (1) in the $n \gg 1$ limit, when the parameters κ and γ can also be related.²³ This expression was obtained in the framework of nonequilibrium thermodynamics and the TE was related with the relaxation of the AFM spin configuration toward equilibrium, which is triggered by the FM magnetization reversal.

Exchange bias is of extreme importance for present day magnetoresistive sensors^{24,25} (spin valves and tunnel junctions)^{26,27} in high density recording media or for biomedical applications. A spin valve (SV) is a magnetic nanostructure constituted by two ferromagnetic (FM) layers separated by a thin nonmagnetic (NM) metallic spacer.²⁶ To fix the magnetization of one of the FM layers (pinned layer), one uses an underlying antiferromagnetic layer. The other FM layer (free layer) rotates when a small magnetic field is applied. Relatively high magnetoresistance (MR) values can be achieved with such SV design, but new ways to enhance MR and device sensitivity are being continuously researched. One such way is the fabrication of a nano-oxide layer (NOL) just above and in the middle of the free and pinned layers, respectively.²⁸ These NOL spin valves can more than double the MR ratio of simpler stacks because of specular reflection of electrons at the FM/NOL interfaces.²⁹ We recently showed that the pinned layer NOL is formed by CoFe oxides that have a paramagnetic/antiferromagnetic transition below room temperature ($T_B \approx 175$ K) that can strongly affect transport properties, particularly MR.^{30–32}

In this work, we present a detailed study on the training effect in MnIr/CoFe/NOL/CoFe/Cu/CoFe/NOL/Ta specular spin valves by using MR(H) measurements (in the 300–15 K temperature range) and different experimental procedures. The training effect was never observed in common non-specular spin valves (without NOLs, but otherwise similar to the studied specular SV). This indicates that the MnIr/CoFe exchange interaction does not evolve with cycling. On the other hand, the exchange field of our specular spin valve is (below T_B) given by two contributions: one arising from the MnIr layer and another from the pinned layer AFM-NOL. Thus, when field cooling under a positive (negative) magnetic field, the NOL ordering at T_B leads to an enhanced (reduced) SV-exchange field.^{31,33} In the specular spin valve, a training effect was observed for $T < 175$ K. We then relate such training effect to the nano-oxide layer AFM ordering and to changes in the corresponding interfacial spin structure with n . The training effect in specular spin valves is characterized not only by the decrease in exchange and coercive fields with cycling but also by the decrease of the giant magnetoresistive (GMR) ratio. The influence of the NOL spin structure on the magneto-transport of the specular spin valves was then studied. Our MR(H) measurements revealed a residual MR value at $H \gg 0$, which will be related to a spin-glass-like behavior of the interfacial magnetism induced by the nano-oxide layer. We also found that TE depends on the applied magnetic cooling field (H_0): For $H_0 \geq 0$, we observed a fairly large TE but the same exchange field in the $n \rightarrow \infty$ limit (H_{exch}^∞ ; independently of H_0). On the other hand, for a negative cooling field, we observed a small TE and different H_{exch}^∞ values for different H_0 . For $H_0 = -500$ Oe, we observe low MR, H_{exch} , and training effect. The temperature dependence of the training effect was experimentally obtained and fitted by using a theoretical model based on free energy considerations.³⁴

II. EXPERIMENTAL DETAILS

A specular spin valve structure was fabricated by using a standard SV inserted between two nano-oxide layers of CoFe. The NOL-SV with the structure Mn₈₃Ir₁₇(90 Å)/Co₉₀Fe₁₀(14 Å)/oxidation/Co₉₀Fe₁₀(15 Å)/Cu(22 Å)/Co₉₀Fe₁₀(40 Å)/oxidation/Ta(30 Å) was grown on a glass substrate by ion beam deposition, post-annealed in vacuum (10^{-6} Torr) at 270 °C for 10 min, and then cooled in a 3 kOe applied field. The resulting exchange bias direction between the MnIr and (pinned) CoFe layer is taken here as the positive direction. CoFe oxidation was performed by using the remote plasma method, for 3 min. Notice, however, that the presence of the Ta capping layer on top of the oxidized free layer leads to differences between the compositions of the two NOLs of our specular spin valve. In fact, we found evidence that the NOL on top of the free layer is formed by paramagnetic oxides through all the studied temperature range. On the other hand, the pinned layer NOL is formed by oxides that antiferromagnetically order below room temperature. Here, this difference is related to the formation of a Ta₂O₅ layer on top of the free layer, as described in more detail below. Electrical resistance and magnetoresis-

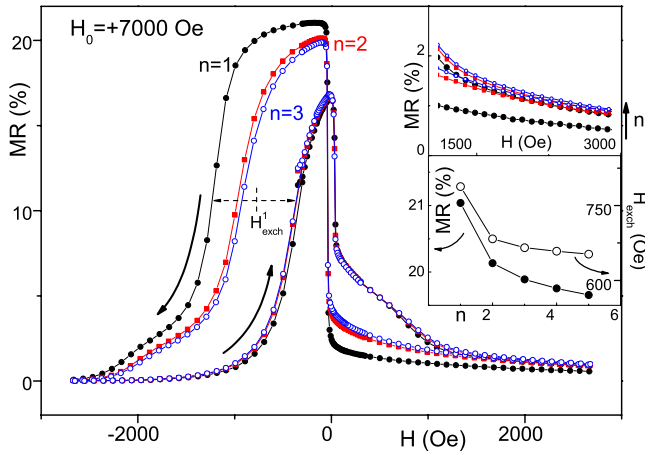


FIG. 1. (Color online) Three $MR(H)$ curves consecutively measured (at $T=15$ K; after FC under $H_0=+7000$ Oe) and displaying the training effect. Upper inset: enlarged $H \gg 0$ region showing an enhanced residual MR with increasing n and thus poorer \Rightarrow parallelism. Lower inset: GMR ratio and exchange field dependence on the number of cycles.

tance were measured with a standard four-point dc method, with a current stable to $1:10^6$ and applied fields of up to 8 kOe and an automatic control and data acquisition system. Temperature dependent measurements were performed in a closed cycle cryostat down to 15 K.³²

To study the training effect, several experimental procedures were used. First, we performed field cooling runs (from 320 K) under different cooling fields H_0 (always applied along the MnIr/CoFe exchange bias direction). At least five consecutive magnetoresistance cycles $MR(H)$ were performed at $T=15$ K before the sample was heated again up to 320 K. We also measured $MR(H)$ cycles at a constant temperature (in the 300–15 K range) after cooling from 320 K under selected H_0 . Finally, we performed measurements in which the sample was cooled from 320 K down to a temperature T_{cool} under a cooling field H_0 . Below T_{cool} , cooling was performed under zero applied magnetic field (for which the FM magnetization points in the positive direction). $MR(H)$ cycles were then measured at the constant low temperature $T=15$ K. The H_{exch} value and its dependence on the measurement procedures was obtained from the $MR(H)$ curves. Here, we define H_{exch} as the shift from zero magnetic field of the $MR(H)$ curve at one-half its maximum value (see Fig. 1). Although $MR(H)$ cycles of spin valves are not as adequate as magnetization hysteresis loops to provide exchange bias values, their sensitivity to small deviations from pinned/free layer collinearity enables the observation of interesting TE-related phenomena, as will be shown below. We could then construct a detailed picture of TE and its dependence on temperature, cooling field and cooling temperature.

We define the training effect TE_n of the exchange field as the relative decrease in H_{exch} from the first to the n th cycle:

$$TE_n = \left(1 - \frac{H_{exch}^1 - H_{exch}^n}{H_{exch}^1} \right) \times 100(\%). \quad (3)$$

The same procedure is used to define changes of the MR ratio with n .

III. EXPERIMENTAL RESULTS AND DISCUSSION

$MR(H)$ measurements in the specular spin valve at room temperature showed no training effect. Consecutive $MR(H)$ cycles displayed equal shape, exchange and pinned layer coercive fields, and GMR ratio. However, with decreasing $MR(H)$ measuring temperature, training effect appeared for $T \approx 150$ K, just below the AFM ordering temperature of the oxides that constitute the pinned layer NOL.³⁰ Consequently, the observed training effect is related to changes in the AFM spin structure of this NOL.

Figure 1 depicts the first three $MR(H)$ cycles measured at $T=15$ K, after field cooling under $H_0=+7000$ Oe. For $n=1$, $MR(H)$ displays a typical SV behavior: low resistance (R) at positive fields, followed by a high R state when the magnetization of the free layer reverses near zero field (antiparallel \rightleftharpoons alignment), and, finally, a decrease to zero MR at large negative fields associated with the reversal of the FM pinned layer (parallel \leftarrow configuration). However, an uncommon characteristic is also seen: MR only slowly goes to zero at large positive fields, denoting incomplete \Rightarrow parallelism. This later feature is related to the effects of the interfacial magnetism of the AFM-NOL formed within the pinned layer, on the corresponding FM magnetization.

Several reasons lead us to attribute this behavior to the influence of the nano-oxide layer formed within the pinned layer on the SV magneto-transport properties and to discard any effects arising from the NOL also present on the top of the free layer. First, we notice that no training effect was observed when small magnetic fields were applied, thus reversing only the magnetization of the free layer. Furthermore, the (small) negative magnetic field at which the free layer reverses (usually due to a magnetic coupling between pinned and free FM layers) and the free layer coercive field show only a monotonous increase as temperature decreases (not shown). If the NOL on top of the free layer antiferromagnetically ordered, one would expect these characteristic fields to significantly vary below the corresponding ordering temperature. Such a significant variation is indeed observed but only for the exchange bias and pinned layer coercive fields below $T_B \sim 175$ K.³¹ We must therefore conclude that the compositions of the two nano-oxide layers are different, with the NOL on top of the free layer formed by paramagnetic oxides in the studied temperature range. We attribute the lack of AFM oxides in the free layer NOL to the formation of a Ta_2O_5 layer through the solid state reaction $CoFeO_x + Ta \rightarrow CoFe + Ta_2O_5$ (notice the Ta capping layer deposited on top of the free layer).³⁵ Such a reaction is expected because the electronegativities (in the Pauling scale) of O, Co, Fe, and Ta are 3.44, 1.88, 1.83 and 1.5, respectively, making ionic bonds between O and Ta more likely than with Co or Fe.³⁵ To confirm this, we have also measured another dual specular SV (with two nano-oxide layers, one within the pinned layer, the other formed by the partial oxidation of the free layer) but without the Ta capping layer. In this case, we indeed found evidences of an AFM ordering of the NOL on top of the free layer, through the large increase of the free layer characteristic fields below room temperature (not shown). However, the existence of two AFM NOLs makes the analysis of the exchange bias and training effect

experimental data difficult, so that we restrict the reported results to the dual specular spin valve with a Ta capping layer. The effects described below will therefore be discussed as due only to changes in the AFM spin structure of the pinned layer NOL.

Returning to Fig. 1, we observe that the $MR(H)$ measurements evolve with n , showing a decrease in the pinned layer switching fields (particularly of the descending H branch) and of the exchange and pinned layer coercive fields. We relate the training effect with the relaxation of the AFM spin structure toward the equilibrium configuration, that results in the partial loss of its net magnetization and of H_{exch} with cycling. Some AFM interfacial spins, originally aligned along the cooling field change their directions and the system falls into another metastable configuration during FM reversal.

Open magnetization hysteresis loops [$M(H)$] were in fact observed in Co_3O_4 nanowires even for strong applied magnetic fields.³⁶ This reveals the loss of magnetization occurring when $M(H)$ cycles are performed and was shown to be a signature of the presence of a spin-glass phase in the AFM interfacial spin structure. It was argued that when the system was field cooled below a freezing temperature, some spins in the spin-glass phase become frozen in the cooling field direction. The frozen spins that keep their direction will then provide pinning force during hysteresis cycle measurements. Notice that the observation of the open $M(H)$ loops in the Co_3O_4 nanowires was only possible because of the large amount of material measured and of the absence of additional FM materials that would mask this effect. A similar observation that use $M(H)$ cycles is therefore very difficult in thin films. An open $M(H)$ loop was also observed in the $\text{Pr}_{1/3}\text{Ca}_{2/3}\text{MnO}_3$ manganite,³⁷ with signatures of interface exchange coupling of FM nanodomains in an AFM background, and was also attributed to the coupling between FM and glasslike surface spins.

The lower inset of Fig. 1 displays the behavior of both the MR ratio (left) and the H_{exch} (right) with cycling. The H_{exch} decrease is more pronounced from the first to the second $MR(H)$ cycles. Subsequent $MR(H)$ cycles show much more attenuated differences. However, we notice that the training effect leads not only to the reduction of the exchange field but also to a lower GMR ratio due to a *smaller* antiparallelism between the magnetizations of the pinned and free layers at SV switching (near $H=0$). In the upper inset of Fig. 1, we observe that the residual magnetoresistance at large positive magnetic fields depends on the number of cycles performed, increasing with increasing n . The lack of full parallelism indicates canted FM spins in the pinned layer strongly coupled to interfacial AFM spins in the negative direction.¹⁹ Thus, we can probe the changes in the net interfacial AFM magnetization and the loss of uncompensated AFM magnetization with n .

The angular dependence of the GMR effect can usually be written as²⁶

$$\text{GMR}(\theta) = \text{GMR}^{\text{max}} \frac{1 - \cos(\theta)}{2}, \quad (4)$$

where GMR^{max} is the maximum GMR obtained when the pinned and free layers are antiparallel and θ is the angle

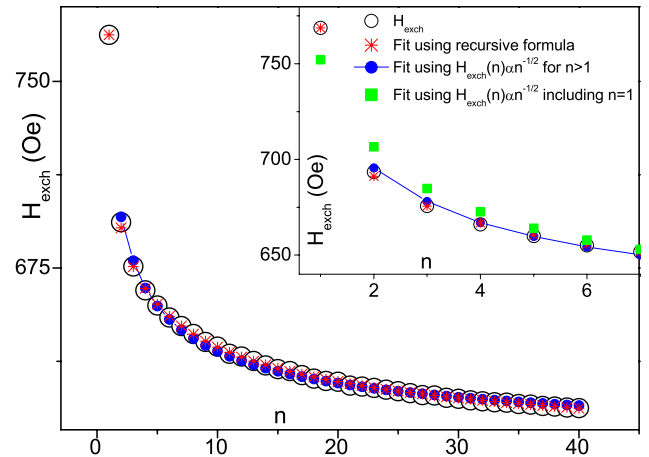


FIG. 2. (Color online) Experimental exchange field (open circles) as a function of $MR(H)$ cycle number (measured at $T = 15$ K after zero field cooling) and fits to the different models presented in the text [Eqs. (1) (for $n > 1$; circles) and (2) (stars)]. The inset shows the region $1 \leq n \leq 7$ and also a fit to Eq. (1) for $n \geq 1$ (squares).

between pinned and free layers. For the experiments shown in Fig. 1 ($\text{GMR}^{\text{max}} \approx 21.0\%$), and using the GMR values at high applied positive fields (0.5% for $n=1$; 0.86% for $n=3$), we estimate angles θ of 17.7° and 23.3° for $n=1$ and $n=3$, respectively. This increase in θ with n shows that the nonsaturating MR is related to the amount of interfacial AFM spins in the negative direction. The reversal of AFM spins with n (lost magnetization) due to the training effect, is then revealed in our MR measurements by the corresponding increase in the θ -angle, i.e., the canted magnetization that does not become aligned with the maximum applied magnetic field, being a convincing indication of the spin-glass-like behavior of the interfacial magnetism induced by the nanoxide layer. Such a spin glass behavior should arise from randomness and frustration in magnetic interactions due to roughness at the AFM/FM interface. Notice that $M(H)$ cycles could not reveal any sign of such open loop behavior in our samples, being an indication of the smallness of the lost magnetization.³⁸ In contrast, GMR measurements, being very sensitive to small deviations from parallelism between pinned and free layers, provide an excellent tool to qualitatively probe even a small interfacial magnetization loss.

The spin-glass-like nature of the AFM spin structure was also reported in $\gamma\text{-Fe}_2\text{O}_3$ coated Fe nanoparticles,^{18,39} wherein a nonsaturation of the magnetic moment was observed in fields up to 5 T; in CoO nanoparticles,^{40,41} where the origin of exchange bias was attributed to pinning of the FM magnetization to a spin-glass-like state of uncompensated AFM spins with high anisotropy; and in exchange bias FeNi/FeMn bilayers,⁴² wherein the obtained magnetic properties were similar to those of disordered interfaces.

Figure 2 shows the evolution of the exchange field for a large number of cycles (open circles). The corresponding $MR(H)$ curves were measured at $T=15$ K after zero field cooling. After 40 cycles, the exchange field decreases to $\sim 80\%$ of its initial value, revealing the importance of the contribution of the pinned layer AFM-NOL to the overall

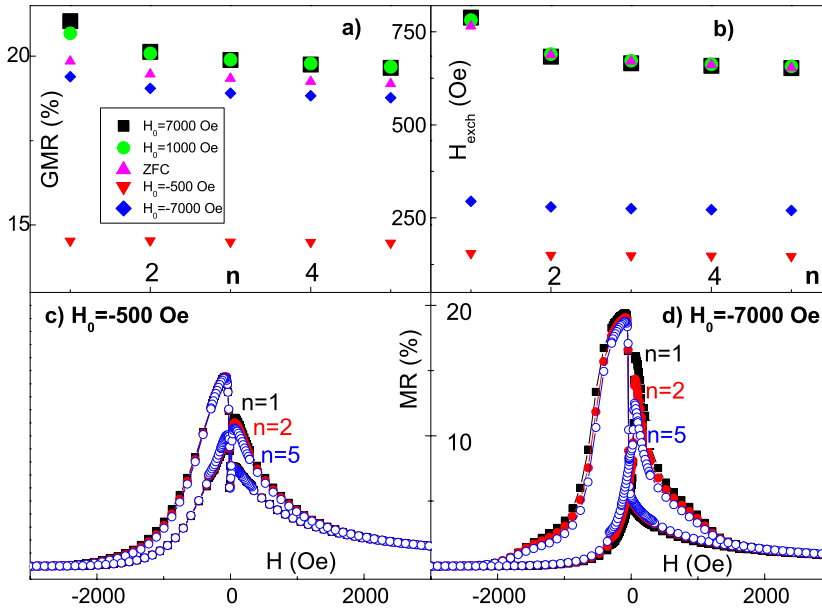


FIG. 3. (Color online) Dependence of (a) GMR ratio and (b) H_{exch} on the number of MR(H) cycles performed ($n \leq 5$) at 15 K for several cooling fields. MR(H) cycles obtained at $T = 15$ K after field cooling from 320 K under (c) $H_0 = -500$ Oe and (d) $H_0 = 7000$ Oe.

exchange field (MnIr+NOL). After fitting our data to the models presented above, it is clear that the recursive relation [Eq. (2)] gives a good correlation with the experimental results for all n values (stars). The same does not occur in the limit of small cycling when the empirical relation [Eq. (1)] is used (full circles; see also inset of Fig. 2).

Recently, the term $-\gamma_c(H_{\text{exch}}^n - H_{\text{exch}}^\infty)^5$ was added to Eq. (2), originating from a higher order expansion of the free energy of the system.⁴³ We have also fitted our experimental data to this extended expression (not shown). However, only a marginal improvement (of less than 1%) on the fitting quality was found. Furthermore, the γ value remained virtually unchanged when compared to that obtained by using Eq. (2) and we found that $\gamma_c \ll \gamma$. This indicates that the use of the expanded expression is not justified in our system.

Field cooling from 320 K down to 15 K with different cooling fields revealed that the SV-exchange bias strongly varies with H_0 [see the $n=1$ data in Fig. 3(b)]. For $H_0 \geq 0$, the pinned layer magnetization is aligned along the positive direction (\rightarrow), resulting in enhanced H_{exch} when NOL ordering occurs. For $H_0 \ll 0$, the FM-pinned layer magnetization is aligned with the applied magnetic field (\leftarrow) and reduced H_{exch} is then observed. After $H_0 = -500$ Oe cooling runs are performed, we obtain low magnetoresistance ratio and exchange field. Also, the corresponding MR(H) cycles [Fig. 3(c)] show an anomalous behavior, with the absence of the usual plateau of constant high resistance corresponding to antiparallel pinned/free layer magnetizations. The shapes of the obtained curves are characteristic of MR(H) cycles performed with H misaligned with the exchange bias direction. The $H_0 = -500$ Oe case is then peculiar and will be discussed in detail below. Notice that the exchange bias arising from the MnIr layer (sign and magnitude) is not affected by the field cooling procedures.

The training effect also depends on the cooling field H_0 , as depicted in Fig. 3. The GMR ratio decreases with cycling ($n \leq 5$) for all cooling fields except for $H_0 = -500$ Oe, for which a practically constant GMR = 14.5% is obtained [Figs. 3(a) and 3(c)]. The same occurs for the exchange field [Fig.

3(b)]. Although a fairly large TE_5 ($\sim 80\%$) is observed for $H_0 \geq 0$, much smaller TE occurs for both $H_0 = -500$ Oe and $H_0 = -7000$ Oe [$\sim 95\%$ and $\sim 93\%$, respectively; see Figs. 3(c) and 3(d)]. H_{exch} extrapolates to the same value in the limit of large number of cycles for all $H_0 \geq 0$ [H_{exch}^∞]. However, different values of H_{exch}^∞ are clearly obtained for negative H_0 .

The dependence of H_{exch}^∞ on the cooling field H_0 can also be an indication that several stable configurations are available for the spin structure of the magnetically disordered AFM-NOL, depending on the magnetic history of the sample.^{36,44} When our system is cooled below the NOL-blocking temperature, a spin configuration is chosen among the many available metastable states.⁴⁵ Thus, depending on the cooling field and cooling temperature (see below), different spin configurations can be reached by the system.

For $H_0 \geq 0$ [Fig. 3(c)], the exchange bias tends to the same value, likely reflecting the evolution of the interfacial AFM magnetic structure to similar configurations. On the other hand, if a negative cooling field is applied, the NOL domain structure evolves with n to completely different configurations. The smaller TE observed for $H_0 < 0$ indicates that in this case, the field cooled domain structure is very close to the local energy minimum the system evolves to. Varying the cooling field thus leads to changes in the interface magnetic configuration and to different exchange bias fields.

Let us now consider the particular $H_0 = -500$ Oe situation. In this case, the pinned layer magnetization is not (at least homogeneously) aligned with the applied magnetic field. This is clearly visible in Fig. 4, wherein we display $R(T)$ curves measured under $H = -500$ Oe and for parallel (P; low resistance) and antiparallel (AP; high resistance) pinned/free layer magnetizations. The P and AP curves were taken from MR(H) measurements performed at constant temperatures after field cooling under $H_0 = 3000$ Oe. For $H = -500$ Oe, the measured electrical resistance is clearly different from both P and AP situations. The magnetization of the FM pinned layer then does not lie along the applied

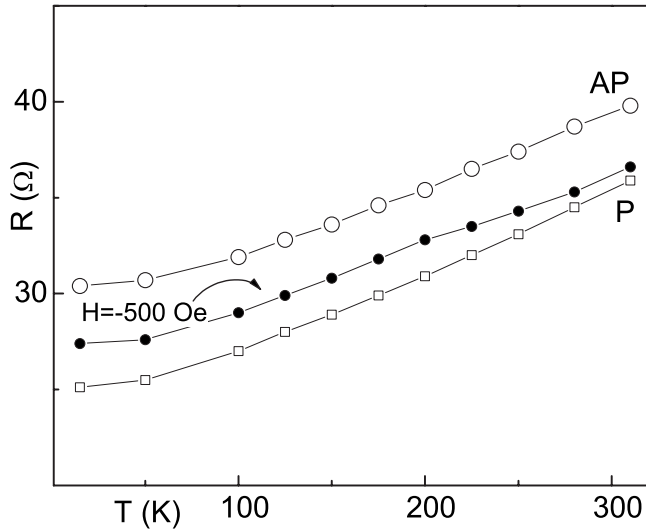


FIG. 4. Temperature dependence of the electrical resistance of the studied specular spin valve in the parallel (P), antiparallel (AP), and after field cooling under $H_0 = -500$ Oe.

negative magnetic field (due to the presence of domains in the pinned layer and/or to coherent rotation of the pinned layer magnetization away from the applied field direction). Note that it is the FM magnetization state (that, in turn, does depend on the applied magnetic field) that defines the interface coupling between the AFM and FM layers and not the cooling field itself.⁴⁶ The exchange bias is locally determined by the FM magnetization state and domains in the FM lead to an exchange bias that is an average over the domain magnetization directions, as obtained upon field cooling under $H_0 = -500$ Oe.⁴⁷ Thus, when crossing $T_B \approx 175$ K under $H_0 = -500$ Oe, we expect a complex domain structure to be formed in the AFM nano-oxide layer. Subsequent MR(H) cycles measured at 15 K show an anomalous behavior [Fig. 3(c)], which is a characteristic of the cycles performed with the applied magnetic field making an angle with the exchange bias direction. Since the MR(H) cycles were measured with H applied in the same direction of H_0 , we con-

clude that the AFM-NOL interfacial net magnetization does not lie along the H_0 direction. The surprisingly small training effect observed for this case indicates that the interfacial spin state is almost unaffected by the field cycling (see below).

In Figs. 5(a) and 5(b), we observe the GMR ratio and H_{exch} versus n for several temperatures from 300 to 15 K ($H_0 = 3000$ Oe). As expected, the MR ratio and H_{exch} increase with decreasing temperature. We also notice the absence of TE down to $T = 175$ K, for which both MR and H_{exch} basically retain their initial $n = 1$ value with cycling [see the dashed lines in Figs. 5(c) and 5(d), which represent the 100% TE level]. However, for $T = 150$ K, we already observe $\text{TE}_5 \sim 95\%$. Furthermore, TE_5 increases with decreasing temperature ($\text{TE}_5 \sim 83\%$ for $T = 15$ K). Binek *et al.*³⁴ developed a phenomenological theory that allowed the explicit determination of the temperature dependence of the training effect in exchange biased systems in terms of $\gamma = \gamma(T)$. By using Eqs. (7) and (8) of Ref. 34, we were able to well fit our $\gamma(T)$ data (Fig. 6). Note that large (small) γ values are related to small (large) training effects. The obtained low value of γ at low temperatures indicates that, due to the lack of thermal excitations, there is no thermally driven change in H_{exch} .

The model of Binek *et al.*³⁴ considers the training effect within the framework of relaxation phenomena, by using a discretized Landau-Khalatnikov equation. The reversal of the FM magnetization is the driving force that leads (in the $n \rightarrow \infty$ limit) the AFM interfacial magnetization toward equilibrium or a pronounced local minimum of the free energy. Some frozen AFM spins, which are initially along the cooling field direction, change direction with the FM reversal and the system goes into another metastable state, with a lower net magnetization and, consequently, a lower H_{exch} . The fact that our data could be well fitted by using the mentioned model indicates the correctness of the spin configurational relaxation model.

Figure 7 shows the training effect of the exchange field for different cooling temperature for $H_0 = 3000$ Oe (solid symbols) and $H_0 = -500$ Oe (open symbols). Recall that below T_{cool} , cooling is performed under zero magnetic field and that all MR(H) measurements are then performed at T

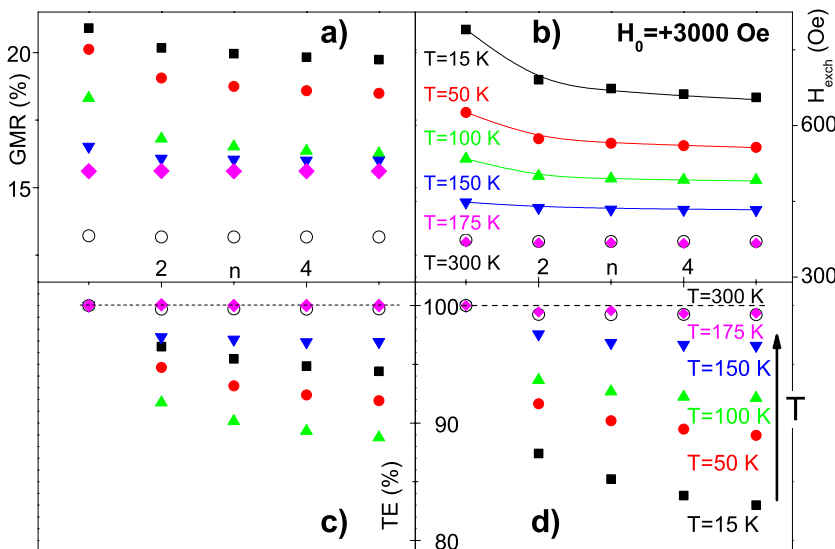


FIG. 5. (Color online) Dependence of the (a) GMR ratio and (b) H_{exch} on the number of MR(H) cycles performed for several temperatures and corresponding training effect [(c) and (d)]. MR(H) measurements were performed after field cooling under $H_0 = 3000$ Oe from 320 K. Corresponding fits to Eq. (2) are displayed as lines in (b).

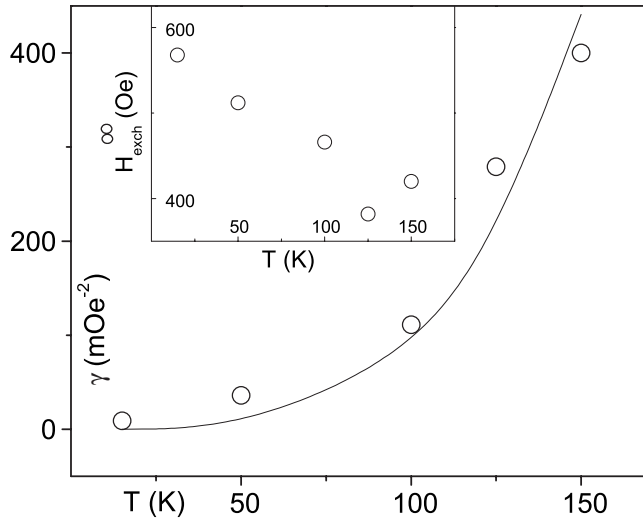


FIG. 6. Temperature dependence of the γ parameter and corresponding fit (line). Also displayed is the $H_{\text{exch}}^{\infty}(T)$ behavior (inset).

= 15 K. For $H_0 = +3000$ Oe, TE slightly increases with decreasing T_{cool} [Fig. 7(b)]. Since cooling with decreasing T_{cool} in a large positive field favors a net positive (\rightarrow) magnetization in the AFM NOL, the observed increase in TE with decreasing T_{cool} shows that the (preferentially positive) AFM spin structure is not stable and the AFM layer tends to rearrange to lower the energy of the system. On the other hand, TE decreases with decreasing T_{cool} for $H_0 = -500$ Oe [Fig. 7(b)]. Since higher T_{cool} experiments induce a higher positive (\rightarrow) net magnetization in the AFM-NOL, it is their reversal that again causes an enhanced training effect. Further notice that different cooling temperatures lead to different H_{exch}^{∞} [Fig. 7(a)], again indicating different stable configurations in the AFM domain structure with similar energies.

As stated above, our MR(H) curves [Fig. 3(c)] indicate that the AFM-NOL pinning direction does not lie along H_0 after field cooling under $H_0 = -500$ Oe. These MR(H) cycles were, thus, obtained with H (applied along H_0) misaligned with the NOL-pinning direction. In this case, the pinned layer FM reversal should proceed by magnetization rotation, instead of domain wall motion that is usual for collinear applied magnetic field and exchange bias direction.⁴⁸ The almost symmetric magnetization reversal processes for the ascending and descending MR(H) branches that then occurs⁴⁹ leads to the very small training effect observed and the sharp TE decrease with decreasing T_{cool} [Fig. 7(b)]. The training effect is then strongly dependent on the angle between the applied magnetic field and the pinning direction and on the FM reversal mechanism.⁴⁸ Further note that some degree of twisting of the magnetization of the pinned layer⁵⁰ may also be induced after field cooling under high negative fields, which would also explain the smaller training effect observed for $H_0 \ll 0$, when compared to that of positive cooling fields.

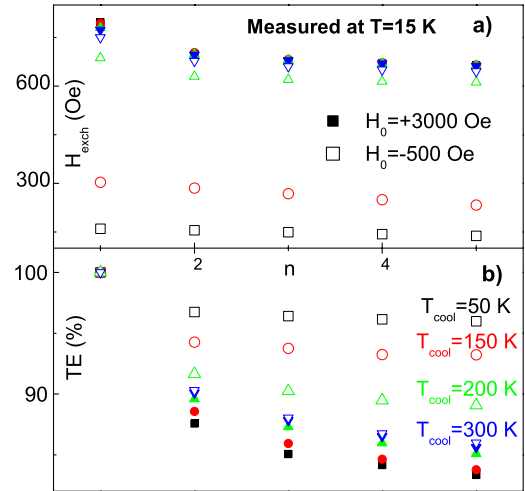


FIG. 7. (Color online) (a) Dependence of H_{exch} on the number of MR(H) cycles performed for several cooling temperatures and (b) corresponding training effect. MR(H) measurements were performed at $T = 15$ K after field cooling under $H_0 = 3000$ Oe (solid symbols) and $H_0 = -500$ Oe (open symbols) from 320 K.

IV. CONCLUSIONS

We presented a detailed study on the training effect of MnIr/CoFe/NOL/CoFe/Cu/CoFe/NOL specular spin valves in the 300–15 K temperature range. The paramagnetic/antiferromagnetic transition of the oxides that form the pinned layer NOL at $T \sim 175$ K lead to a wealth of new phenomena. After field cooling runs under positive (negative) H_0 , we observed enhanced (reduced) H_{exch} . The MR(H) cycles obtained after $H_0 = -500$ Oe showed an anomalous behavior, which is characteristic of MR(H) curves obtained when H is misaligned with the exchange bias direction. The training effect was only observed for $T < 175$ K and was then related with variations in the NOL spin structure with n . We observed that the giant magnetoresistive ratio is strongly influenced by magnetic disorder in the NOL, thus providing strong experimental evidence for the role of noncollinear configurations for MR. We also studied the training effect dependence on magnetic cooling field, measuring temperature and cooling temperature and obtained evidence of the spin-glass nature of the NOL-AFM domain structure. The temperature dependence of the training effect was experimentally obtained and fitted by using a theoretical model based on free energy considerations.

ACKNOWLEDGMENTS

This work was supported in part by Contracts No. FEDER-POCTI/0155, No. POCTI/CTM/36489/2000, No. POCTI/CTM/45252/02, and No. POCTI/CTM/59318/2004 from FCT and Contract No. IST-2001-37334 (NEXT MRAM projects). The authors acknowledge funding from FCT through the Associated Laboratory—IN. J.V. is thankful for a FCT grant (SFRH/BPD/21634/2005).

*joventur@fc.up.pt

†jbsousa@fc.up.pt

‡pfreitas@inesc-mn.pt

- ¹W. H. Meiklejohn and C. P. Bean, *Phys. Rev.* **102**, 1413 (1956).
- ²J. Nogués and I. K. Schuller, *J. Magn. Magn. Mater.* **192**, 203 (1999).
- ³N. C. Koon, *Phys. Rev. Lett.* **78**, 4865 (1997).
- ⁴D. Mauri, H. C. Siegmann, P. S. Bagus, and E. Kay, *J. Appl. Phys.* **62**, 3047 (1987).
- ⁵J.-V. Kim and R. L. Stamps, *Phys. Rev. B* **71**, 094405 (2005).
- ⁶T. C. Schulthess and W. H. Butler, *Phys. Rev. Lett.* **81**, 4516 (1998).
- ⁷A. P. Malozemoff, *Phys. Rev. B* **35**, 3679 (1987).
- ⁸D. V. Dimitrov, S. Zhang, J. Q. Xiao, G. C. Hadjipanayis, and C. Prados, *Phys. Rev. B* **58**, 12090 (1998).
- ⁹P. Miltényi, M. Gierlings, J. Keller, B. Beschoten, G. Güntherodt, U. Nowak, and K. D. Usadel, *Phys. Rev. Lett.* **84**, 4224 (2000).
- ¹⁰U. Nowak, K. D. Usadel, J. Keller, P. Miltényi, B. Beschoten, and G. Güntherodt, *Phys. Rev. B* **66**, 014430 (2002).
- ¹¹J. Keller, P. Miltényi, B. Beschoten, G. Güntherodt, U. Nowak, and K. D. Usadel, *Phys. Rev. B* **66**, 014431 (2002).
- ¹²F. Radu, A. Westphalen, K. Theis-Bröhl, and H. Zabel, *J. Phys.: Condens. Matter* **18**, L29 (2006).
- ¹³J. McCord, R. Schäfer, R. Mattheis, and K.-U. Barholz, *J. Appl. Phys.* **93**, 5491 (2003).
- ¹⁴K. Takano, R. H. Kodama, A. E. Berkowitz, W. Cao, and G. Thomas, *Phys. Rev. Lett.* **79**, 1130 (1997).
- ¹⁵W. J. Antel, Jr., F. Perjeru, and G. R. Harp, *Phys. Rev. Lett.* **83**, 1439 (1999).
- ¹⁶P. Kappenberger, S. Martin, Y. Pellmont, H. J. Hug, J. B. Kortright, O. Hellwig, and E. E. Fullerton, *Phys. Rev. Lett.* **91**, 267202 (2003).
- ¹⁷H. Ohldag, A. Scholl, F. Nolting, E. Arenholz, S. Maat, A. T. Young, M. Carey, and J. Stöhr, *Phys. Rev. Lett.* **91**, 017203 (2003).
- ¹⁸R. K. Zheng, G. H. Wen, K. K. Fung, and X. X. Zhang, *Phys. Rev. B* **69**, 214431 (2004).
- ¹⁹S. Brems, D. Buntinx, K. Temst, C. van Haesendonck, F. Radu, and H. Zabel, *Phys. Rev. Lett.* **95**, 157202 (2005).
- ²⁰F. Radu, M. Etzkorn, R. Siebrecht, T. Schmitte, K. Westerholt, and H. Zabel, *Phys. Rev. B* **67**, 134409 (2003).
- ²¹T. Hauet, J. A. Borchers, P. Mangin, Y. Henry, and S. Mangin, *Phys. Rev. Lett.* **96**, 067207 (2006).
- ²²A. Hochstrat, C. Binek, and W. Kleemann, *Phys. Rev. B* **66**, 092409 (2002).
- ²³C. Binek, *Phys. Rev. B* **70**, 014421 (2004).
- ²⁴M. Rickart *et al.*, *J. Appl. Phys.* **95**, 6317 (2004).
- ²⁵P. P. Freitas, R. Ferreira, S. Cardoso, and F. Cardoso, *J. Phys.: Condens. Matter* **19**, 165221 (2007).

- ²⁶B. Dieny, V. S. Speriosu, S. S. P. Parkin, B. A. Gurney, D. R. Wilhoit, and D. Mauri, *Phys. Rev. B* **43**, 1297 (1991).
- ²⁷J. S. Moodera, L. R. Kinder, T. M. Wong, and R. Meservey, *Phys. Rev. Lett.* **74**, 3273 (1995).
- ²⁸A. Veloso, P. P. Freitas, P. Wei, N. P. Barradas, J. C. Soares, B. Almeida, and J. B. Sousa, *Appl. Phys. Lett.* **77**, 1020 (2000).
- ²⁹L. Wang, J. J. Qiu, W. J. McMahon, K. B. Li, and Y. H. Wu, *Phys. Rev. B* **69**, 214402 (2004).
- ³⁰J. O. Ventura, J. B. Sousa, M. A. Salgueiro da Silva, P. P. Freitas, and A. Veloso, *J. Appl. Phys.* **93**, 7690 (2003).
- ³¹J. O. Ventura, J. B. Sousa, P. P. Freitas, and A. Veloso, *J. Magn. Magn. Mater.* **272-276**, 1892 (2004).
- ³²J. Ventura, J. P. Araujo, J. B. Sousa, A. Veloso, and P. P. Freitas, *J. Appl. Phys.* **101**, 113901 (2007).
- ³³M. Doi, M. Izumi, H. Endo, H. M. Fuke, H. Iwasaki, and M. Sahashi, *IEEE Trans. Magn.* **41**, 2932 (2005).
- ³⁴C. Binek, X. He, and S. Polisetty, *Phys. Rev. B* **72**, 054408 (2005).
- ³⁵F. Shen, Q. Y. Xu, G. H. Yu, W. Y. Lai, Z. Zhang, Z. Q. Lu, G. Pan, and A. Al-Jibouri, *Appl. Phys. Lett.* **80**, 4410 (2002).
- ³⁶E. L. Salabas, A. Rumpelcker, F. Kleitz, F. Radu, and F. Schuth, *Nano Lett.* **6**, 2977 (2006).
- ³⁷D. Niebieskikwiat and M. B. Salamon, *Phys. Rev. B* **72**, 174422 (2005).
- ³⁸J. B. Sousa, J. O. Ventura, M. A. Salgueiro da Silva, P. P. Freitas, and A. Veloso, *J. Appl. Phys.* **91**, 5321 (2002).
- ³⁹B. Martinez, X. Obradors, L. Balcells, A. Rouanet, and C. Monty, *Phys. Rev. Lett.* **80**, 181 (1998).
- ⁴⁰D. L. Peng, K. Sumiyama, T. Hihara, S. Yamamuro, and T. J. Konno, *Phys. Rev. B* **61**, 3103 (2000).
- ⁴¹M. Gruyters, *Phys. Rev. Lett.* **95**, 077204 (2005).
- ⁴²C. Schlenker, S. S. P. Parkin, J. C. Scott, and K. Howard, *J. Magn. Magn. Mater.* **54-47**, 801 (1986).
- ⁴³S. Sahoo, S. Polisetty, C. Binek, and A. Berger, *J. Appl. Phys.* **101**, 053902 (2007).
- ⁴⁴A. M. T. D. Fiorani, L. Del Bianco, and K. N. Trohidou, *J. Phys.: Condens. Matter* **19**, 225007 (2007).
- ⁴⁵D. Fiorani, L. Del Bianco, A. M. Testa, and K. N. Trohidou, *Phys. Rev. B* **73**, 092403 (2006).
- ⁴⁶C. Binek, S. Polisetty, X. He, and A. Berger, *Phys. Rev. Lett.* **96**, 067201 (2006).
- ⁴⁷A. Paul, C. M. Schneider, and J. Stahn, *Phys. Rev. B* **76**, 184424 (2007).
- ⁴⁸X. P. Qiu, D. Z. Yang, S. M. Zhou, R. Chantrell, K. O'Grady, U. Nowak, J. Du, and X. J. Bai, arXiv:0710.2594 (unpublished).
- ⁴⁹B. Beckmann, U. Nowak, and K. D. Usadel, *Phys. Rev. Lett.* **91**, 187201 (2003).
- ⁵⁰H. Fukuzawa, K. Koi, H. Tomita, H. N. Fuke, H. Iwasaki, and M. Sahashi, *J. Appl. Phys.* **91**, 6684 (2002).